Modeling of Centrifugal Stress and Deformation of Double V and Delta Layer of Interior Permanent Magnet Rotor Design-Application to Electrical Vehicles

Hung Bui Duc[1], Dinh Bui Minh[1], and Vuong Dang Quoc[1,*]

ARTICLE INFO

Article history:
Received: 23 February 2022
Revised: 24 March 2022
Accepted: 31 March 2022

Keywords:
IPM motor
Centrifugal force
Electromagnetic force
Mechanical stress
Finite element technique

ABSTRACT

Arangement of permanent magnets with double V and delta layer plays an important role for IPM motors. In range of high speeds, rotors are often deformed and displaced by radial forces. The air gap can be changed by the deformation and displacement of outer rotors due to electromagnetic forces affected by magnet arrangements with V or delta shapes. Hence, the magnetic flux density at the air gap will be reduced with angle changse of V magnet layers. In this research, a finite element approach is developed to simulate and investigate the deformation and centrifugal force of various IPM motors. In addition, the mechanical stress and deformation of the segment and bridge area of IPM rotors have to be also investigaed by both the radial and centrifugal forces. Thus, a modelling of electromagnetic and mechanical problems is presented to consider the different rotor structures. The obtained results have been then applied to design an IPM at a high-speed.

1. INTRODUCTION

Nowadays, the IPM motor is one of the best choices for electrical vehicles (EVs) because of the high-power density, peak torque and efficiency [1], [2], [7], [15]. In practices, for a high-speed of the EVs, the mechanical stresse and centrifugal force are very important quantities that need to be taken into account, because the rotor structure can be destroyed/deformed by centrifugal and electromagnetic forces at a very high speed.

In this approach, a finite element technique is presented to investigate the mechanical stress and displacement for the full load condition at a maximum speed of 16000 rpm. The electromagnetic forces on the rotor segment are computed to introduce to a finite element (FE) model. The occurrence of centrifugal force in the rotor of IPM are proposed by two double V (VV) and delta shapes. For a rotor, the bridge and segment area are very important parts that have to be considered in the design. In practices, due to the less leakage flux, the bridge has usually a thin structure to get a better electromagnetic performance. However, it is difficult to operate with the centrifugal forces at a high speed [3], [8]-[10].

For VV and delta shapes of the rotor, each segment is produced a hole to reduce the centrifugal forces and rotor mass. The VV and delta shape topologies are pointed out in Figure 1. By this topology, the attractive, electromagnetic and centrifugal forces need to be considered, where the centrifugal force is defined in the radial direction of the rotor.

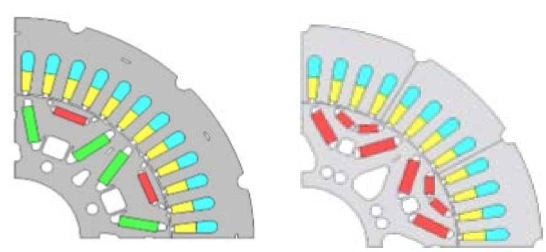

Fig. 1. Topologies of VV and delta shapes.

2. COMPUTATION OF RADIAL MAGNETIC FORCES WITH AIR-GAP DISPLACEMENTS

The change of radial air gap length can be obtained via a mathematical model of the IPM considering both the rotor centrifugal distortion and oval stator deformation. The magnetic flux density at the air gap can be defined via two components of magnetomotive forces (MMFs) in the stator and rotor. In addition, for a high-speed condition, the magnetic flux density at the air gap deformation is considered with the no-load and full load cases. Finally, the centrifugal force is defined by the Maxwell stress tensor technique [5], [11]-[14]. In this approach, the extended formulations are proposed to calculate the components of magnetic fields at the air gap, and the radial forces with different deformations of the air gap. It should be noted that the magnetic fields along the length of air gap plays an

[1]*School of Electrical and Electronic Engineering, Hanoi University of Science and Technology.*
**Corresponding author:* Vuong Dang Quoc; E-mail: vuong.dangquoc@hust.edu.vn.

important role in the formulations. But, the length of air gap taking of the deformation of rotor and stator into account is very complicated during the working of the motor. This means that it is very hard to accurately define the permeance of air gap with a single expression.

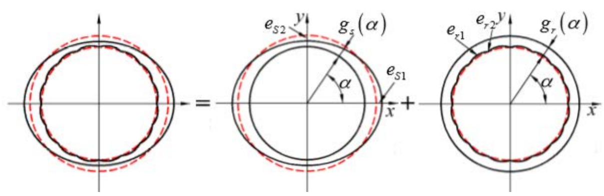

Fig. 2. Deformations of the IPM stator and rotor.

Hence, in order to define the air gap permeance of the IPM motor taking the stator and rotor deformation into account as illustrated in Figure 2, a superposition method is then presented.

A three-phase IPM motor is carried out with a sinusoidal and balanced currents. The radial force variation at the air gap of the oval stator deformation is presented as [4]-[7]

$$g_s(\alpha) \approx -\frac{e_{s1}+e_{s2}}{2}\cos(2\alpha)+g_0$$
$$= -g_0\left[\frac{\delta_{s1}+\delta_{s2}}{2}\cos(2\alpha)-1\right] \quad (1)$$

where, the values (e_{s1} and e_{s2}) are respectively the of maximum and minimum stator deformations, α is the angle of the rotor position, g_0 is the average of air-gap length, and δ_{s1} and δ_{s2} are respectively the elip deformations of stator.

The air-gap length of centrifugal distortion rotor changing around the magnetic circuit periphery is defined as [4]-[7]

$$g_r(\alpha,t) \approx \left(g_0-\frac{e_{r1}+e_{r2}}{2}\right) - \frac{e_{r1}-e_{r2}}{2}\cos[2p(\alpha-\omega_r t)]$$
$$= g_0\left[\left(1-\frac{\delta_{r1}+\delta_{r2}}{2}\right)-\frac{\delta_{r1}-\delta_{r2}}{2}\cos(2p\alpha-2\omega t)\right] \quad (2)$$

and $g_0 = R_{si}-R_{ro}$.

where, δ_{r1}, δ_{r2} are the elip deformations of rotor, e_{r1} and e_{r2} are the air gap lengths, R_{si} and R_{so} are respectively the inner and outer radials of the stator core. For stator deformation, one gets

$$\lambda_{gs}(\alpha) = \frac{1}{-\frac{\delta_{s1}+\delta_{s2}}{2}\cos(2\alpha)+1}$$
$$\approx 1+\frac{\delta_{s1}+\delta_{s2}}{2}\cos(2\alpha)$$
$$= 1+\alpha_{s1}\cos(2\alpha) \quad (3)$$

$$\lambda_{gr}(\alpha,t) = \frac{1}{-\frac{\delta_{r1}-\delta_{r2}}{2}\cos(2p\alpha-2\omega t)+\left(-\frac{\delta_{r1}+\delta_{r2}}{2}+1\right)}$$
$$\approx \frac{\delta_{r1}-\delta_{r2}}{2}\cos(2p\alpha-2\omega t)+\left(1+\frac{\delta_{r1}+\delta_{r2}}{2}\right)$$
$$= 1+\alpha_{r1}\cos(2p\alpha-2\omega t)+\alpha_{r0}, \quad (4)$$

where, p is the number of pole-pairs. For the deformation of rotor, the coefficients (α_{s1} α_{r0}, α_{r1}) are respectively defined as

$$\alpha_{s1} = (\delta_{s1}+\delta_{s2})/2,\ \alpha_{r0} = (\delta_{r1}+\delta_{r2})/2,\ \alpha_{r1} = (\delta_{r1}-\delta_{r2})/2. \quad (5a\text{-}b\text{-}c)$$

The MMF distributions of the stator and rotor carrying with a sinusoidal current quantity can be presented as:

$$F_1(\alpha,t) = \sum_{v=1}^{\infty} F_{mv}\cos(vp\alpha \mp \omega t), \quad (6)$$

$$F_2(\alpha,t) = \sum_{\mu=1}^{\infty} F_{m\mu}\cos(\mu p\alpha \mp \omega_\mu t+\phi_\mu), \quad (7)$$

where, F_{mv} and $F_{m\mu}$ are the MMF magnitudes of the v-*th* and μ-*th* harmonic components for stator and rotor parts.

The centrifugal force on the central bridges is usually produced by the rotation of the rotor. The bilateral bridges of the V-shaped rotor are also introduced to support the central bridges. It schould be noted that the calculation of the centrifugal force on bilateral bridges is more convenient than that on the central bridges. In this context, the V-shaped rotor being equivalent to a central bridge is presented. The VV and delta designs are pointed out in Figure 3. The structure of rotor with spokes is split into several parts, i.e., the inner and outer rings, and spokes. The thickness of the central bridge is equal to spokes, whereas their mass density is suitable with what of the original rotor. The mass density and thickness of the outer ring is computed with an equivalent ring method [6, 7]. For an inner ring thickness, it is similar to what of the rotor yoke. The rotor mass is quite similar to what of the original rotor. The extension of centerline radius (δ_v) of an inner ring caused by the load Y can be defined as [7]

$$\delta_v = \frac{R_v^2 q_v}{A_v E} = \frac{Yn}{A_v 2\pi E} = Yn\lambda_v. \quad (8)$$

The tension N_n in the spokes when the rotor rotates can be obtained

$$N_n = Y - \frac{q_s\omega^2}{2g}(r^2-R_1^2). \quad (9)$$

This deformation is presented as

$$\delta_z = \lambda_z X + \lambda_z' \frac{q_s\omega^2}{2g}R_2^2, \quad (10)$$

where , the terms (λ_s and λ_a') can be defined as:

$$\lambda_s = \frac{1}{A_s E}(R_2-R_1), \quad (11)$$

$$\lambda_a^{'} = \frac{1}{3A_S E}(R_2 - R_1)\left(2 - \frac{R_1}{R_2} - \frac{R_1^2}{R_2^2}\right) \quad (12)$$

For geometric parameters of two IPM motors, the average circumferential force in bilateral bridges and the maximum tensile force in central bridges can be calculated via the above equations.

3. FINITE ELEMENT APPROACH

As presented, the finite element method approach has been developed to simulate and compute performances of the IPM motor. The strong saturation in the rotor bridge and segment areas is also taken into account. The deformation of the rotor bridge has been solved numerically. Thus, the structural finite element model has is pointed out for analysing the centrifigual forces on rotor design. The modelling of IPM motors with VV and Delta shapes are presented in Figure 3. The radial forces with the different speeds and temperatures are pointed out in Figure 4 and Figure 5. For the speed of 16000rpm and over speed of 19200rpm, the phase current of 500Apeak and temperature of 150°C, the force value is approximately 375 Mpa. The most interesting part is the maximum contrifugal force and deformation of the rotor.

The three different cases are now considered, that is: The first one is that the maximum temperature of 150^{0}C degrees is obtained with 20% over the rated speed. This means that the rotation of mechanical rotor in the air is acted by a maximum centrifugal force. The second one is 40% burst speed that rotor rotates in acceleration test.

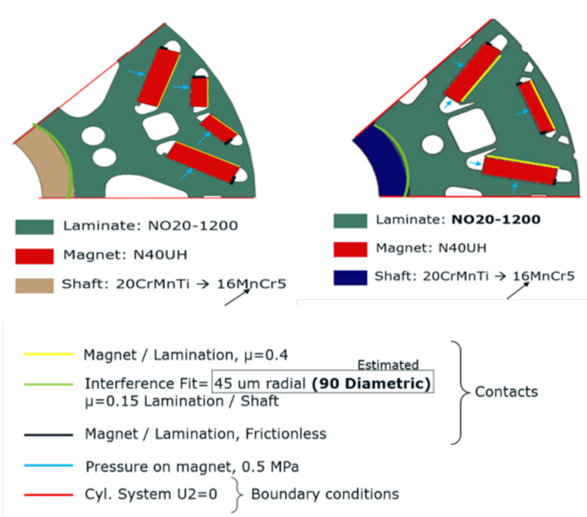

Fig. 3. Modelling of VV and Delta designs.

For a full load case, the maximum centrifugal force for the VV and delta designs are also obtained with 20% over speed of 19200 rpm and 40% burst for a speed of 22400 rpm. The obtained results have shown that the maximum temperature of 150^{0}C at 20% over speed and 40% burst speed conditions. The maximum centrifugal force has appeared all in the segment area. But, the positions of these force are different.

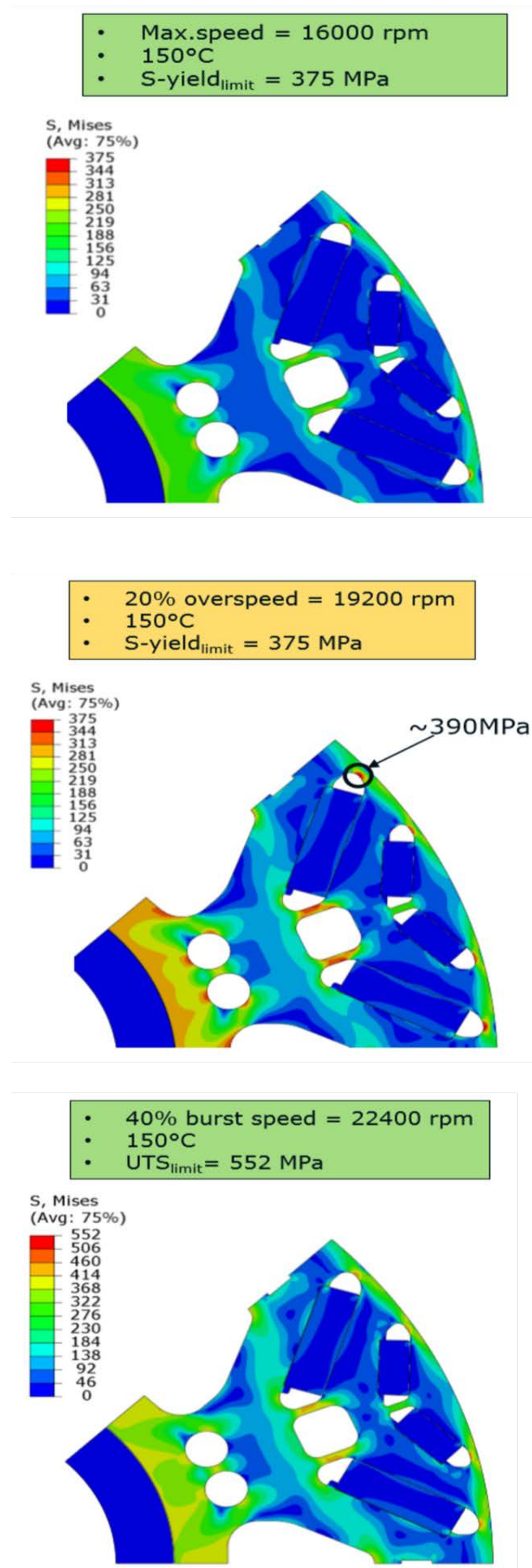

Fig. 4. Stress results of VV design.

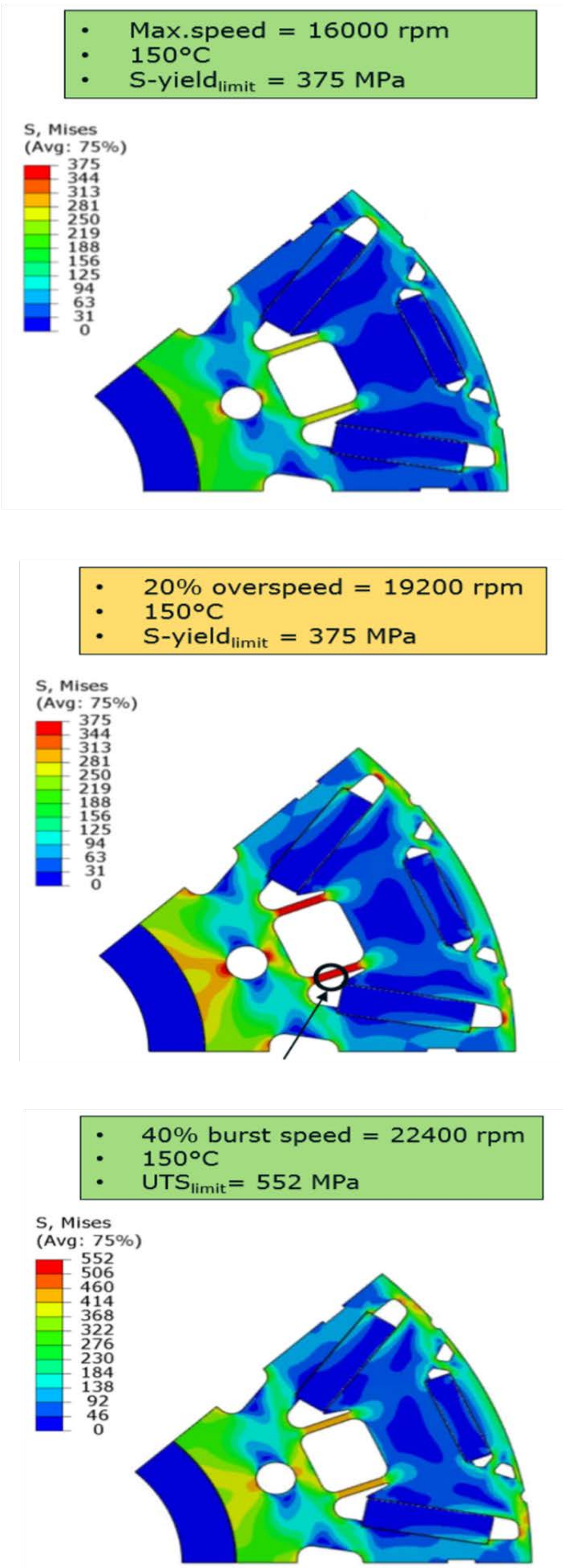

Fig. 5. Stress result of delta design.

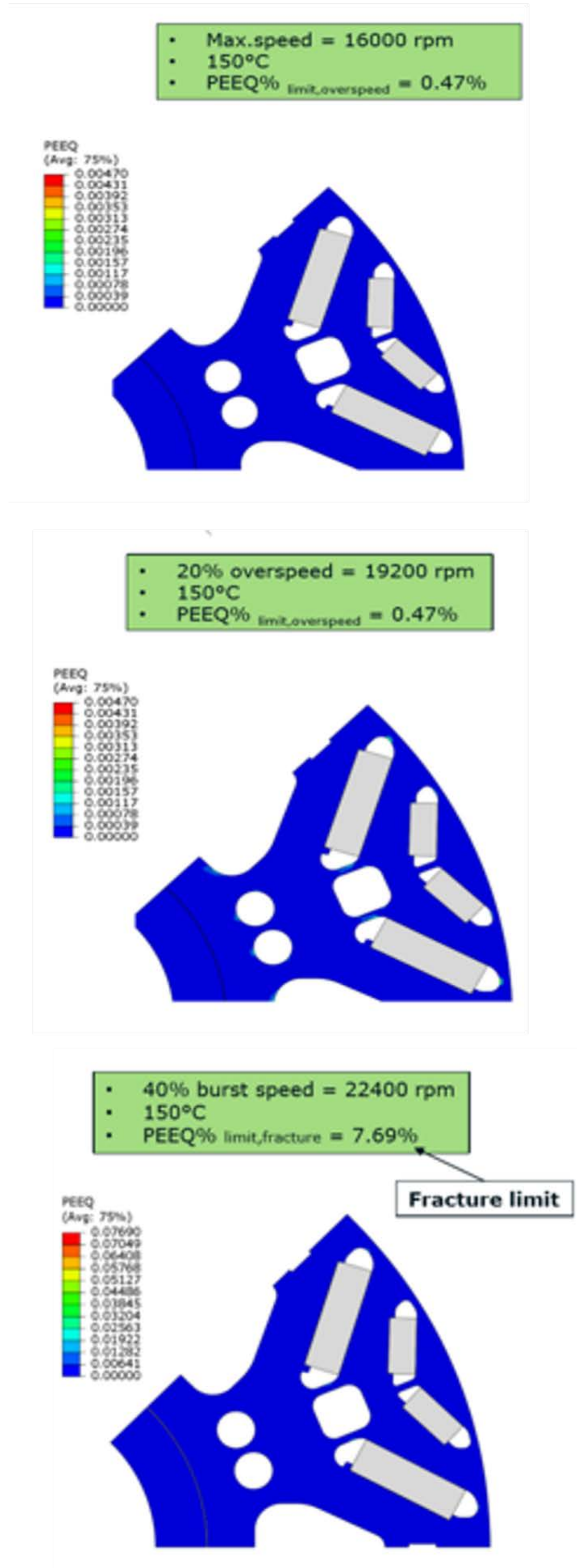

Fig. 6. PEEQ analysis of VV design.

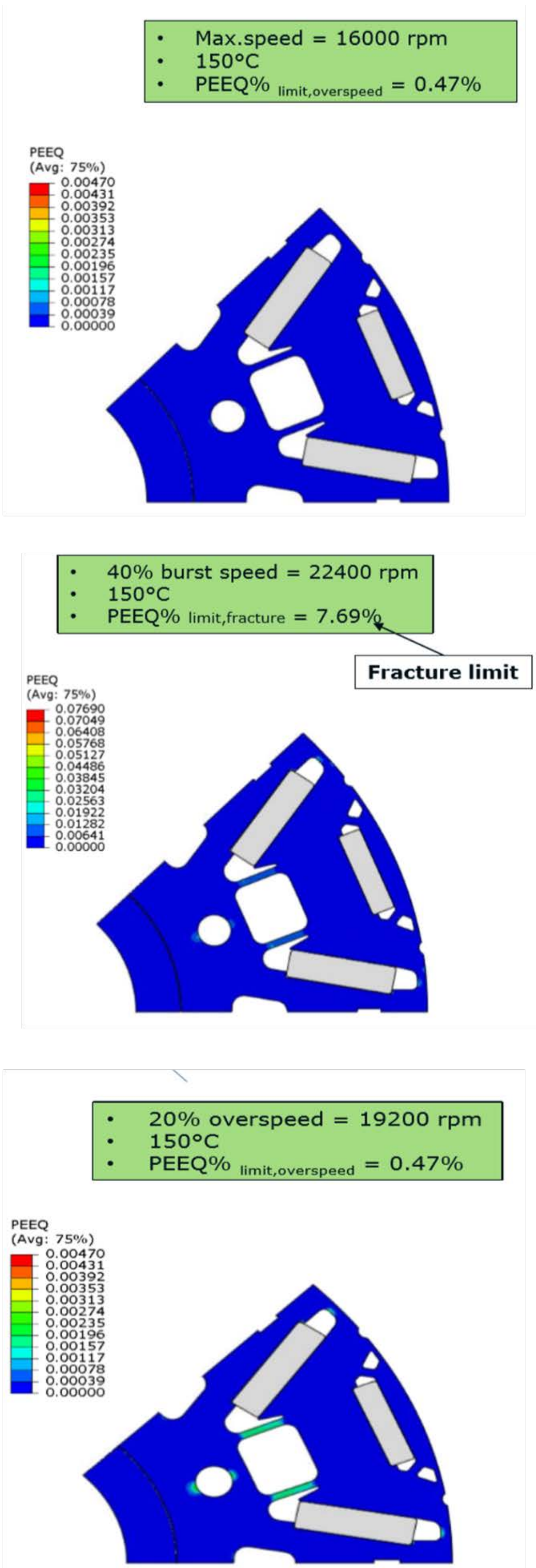

Fig. 7. PEEQ analysis of delta design.

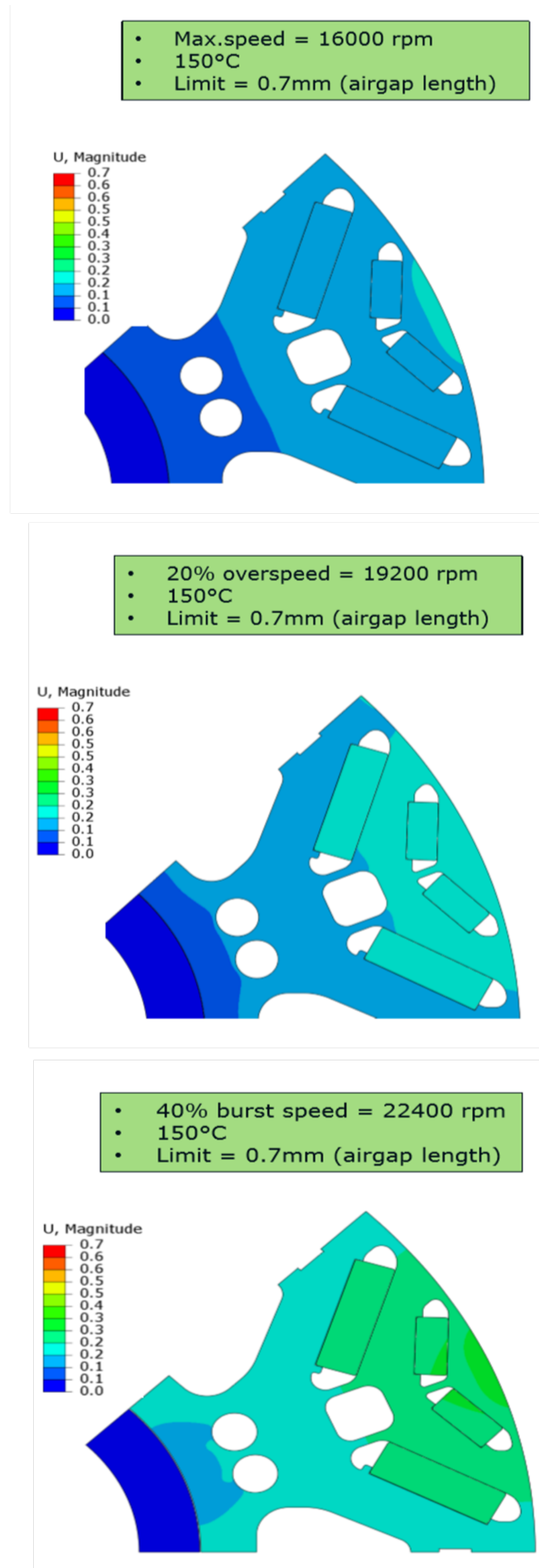

Fig. 8. Validation of displacement VV.

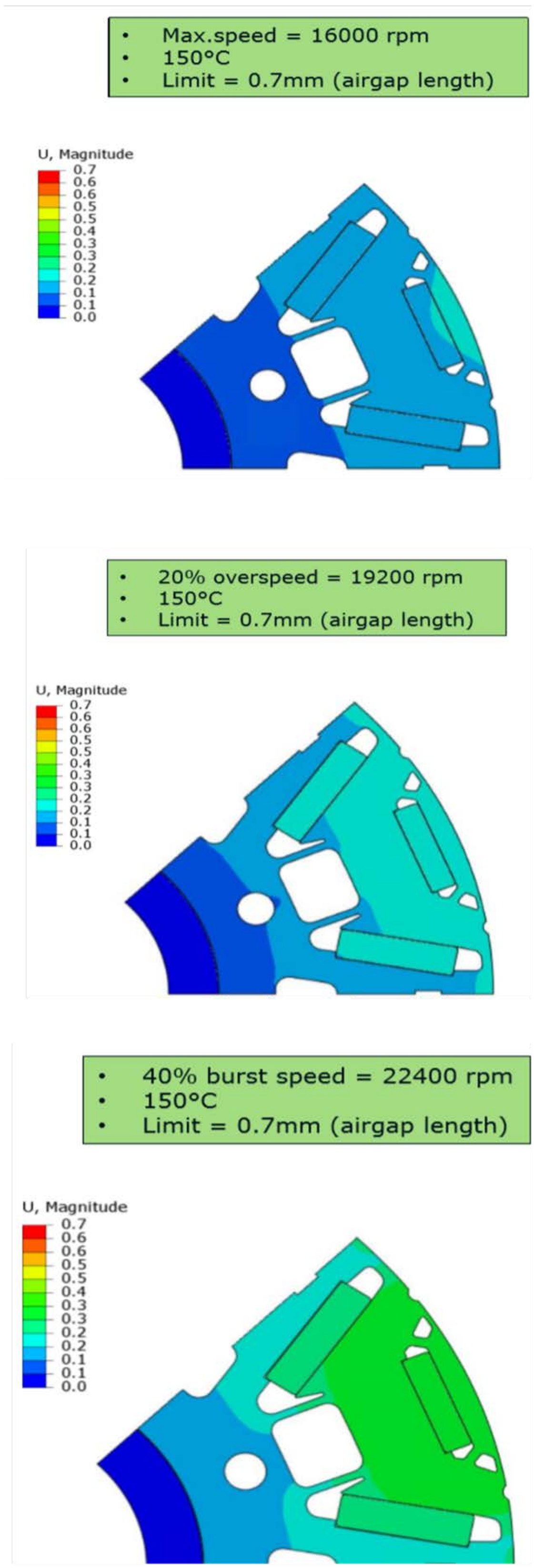

Fig. 9. Validation of displacement delta.

Moreover, for the maximum stress of the V-shape IPM on the outer and inter bridges, it can be obtained with 375 MPa at the speed of 16000rpm on the outer bridge, and 552Mpa at the speed of 22400 rpm on the inter bridge. The power elasticity equivalent (PEEQ) analysis of VV and Delta designs are pointed out in Figure 6 and Figure 7. It is shown that there are no plastification at over speed above design limits and no fracture due to elongation or stress at burst speed.

In particular, the centrifugal forces is the most important part in the stresses and deformation influenced directly by the attraction and electromagnetic forces. The validations of displacement VV and Delta are presented in Figure 8 and Figure 9. The attraction forces help to counteract the stresses on bridges. The displacement of VV shape is around 45µm rad, and its dimention is 90µm under a maximum temperature of 150°C, which is less than the limit level. This means that there is no plasticity at over speed above design limits and no fracture due to elongation or stress at burst speeed. By considering the two rotor models, it can show that the VV shape has less deformation distribution than the delta design.

4. CONCLUSION

In this article, the forces, such as electromagnetic and centrifugal forces in the rotor have been succesfully simulated and computed. The developed method has been proposed to increase the forces on the bridges. It is shown that width of bridges has significant affects directly to the electromagnetic performances. The use of bridges will help the V-shape rotor to operate with several forces. In addition, by producing a hole on the segment, it is a good solution to reduce mechanical forces. This is also shown the marked advantages in the structural analysis. However, it can operate with several mechanical stresses, but its cost is completely higher. Significantly, an express computation and validation of VV and delta designs for the practical IPM motors have been shown.

ACKNOWLEDGMENTS

This research is funded by Hanoi University of Science and Technology under project number T2022-PC-009.

REFERENCES

[1] Di, C.; Bao, X.; Wang, H.; Lv, Q.; He, Y. Modeling and analysis of unbalanced magnetic pull in cage induction motors with curved dynamic eccentricity. IEEE Trans. Magn. 2015, 51, 8106507.

[2] Chai, F.; Li, Y.; Liang, P.; Pei, Y. Calculation of the maximum mechanical stress on the rotor of interior permanent-magnet synchronous motors. IEEE Trans. Ind. Electron. 2016, 63, 3420–3432.

[3] K.J. Lee, K.C. Kim, J. Lee, “Bridge optimization of interior permanent magnet motor for hybrid electric vehicle.” Magnetics Conference, 2003. INTERMAG 2003. [7] K.J. Lee, K.C. Kim, J. Lee, “Rotor optimization of interior permanent magnet synchronous motor considering

mechanical stress" Magnetics Conference, 2005. INTERMAG Asia 2005.

[4] L. Meng, Y.L. Luo, X.F Liu, J.F. Yang, Y.B. Chi, "A Case Study of Electromagnetic Force Distribution on Rotor Core Surface of Turbogenerator." Proceedings of the Chinese Society for Electrical Engineering, vol.25. No.1. Jan. 2005

[5] Park, J.K.; Hur, J. Detection of inter-turn and dynamic eccentricity faults using stator current frequency pattern in IPM-type BLDC motors. IEEE Trans. Ind. Electron. 2016, 63, 1771–1780.

[6] Zuo, S.; Lin, F.; Wu, X. Noise analysis, calculation, and reduction of external rotor permanent-magnet synchronous motor. IEEE Trans. Ind. Electron. 2015, 62, 6204–6212.

[7] Mingqiao Wang;Haotian Zhu;Chengyu Zhou;Ping Zheng;Chengde Tong,"Analysis and Optimization of a V-Shape Combined Pole Interior Permanent-Magnet Synchronous Machine With Temperature Rise and Demagnetization Considered", IEEE Access Year: 2021 | Volume: 9 | Journal Article | Publisher: IEEE.

[8] Guanghui Du;Wei Xu;Jianguo Zhu;Na Huang,"Power Loss and Thermal Analysis for High-Power High-Speed Permanent Magnet Machines" IEEE Transactions on Industrial Electronics, Year: 2020 | Volume: 67, Issue: 4 | Journal Article | Publisher: IEEE.

[9] E. Armando, P. Guglielmi, G. Pellegrino, M. Pastorelli, and A. Vagati, "Accurate Modeling and Performance Analysis of -PMASR Motors," IEEE Trans. Ind. Appl., vol. 45, no. 1, January/February 2009.

[10] Dong-Kuk Lim;Kyung-Pyo Yi;Dong-Kyun Woo;Han-Kyeol Yeo;Jong-Suk Ro;Cheol-Gyun Lee;Hyun-Kyo Jung,"Analysis and Design of a Multi-Layered and Multi-Segmented Interior Permanent Magnet Motor by Using an Analytic Method" IEEE Transactions on Magnetics Year: 2014 | Volume: 50, Issue: 6 | Journal Article | Publisher: IEEE.

[11] G. Pellegrino, A. Vagati, and P. Guglielmi, and B. Boazzo, "Performance Comparison between Surface-Mounted and Interior PM Motor Drives for Electric Vehicle Application," IEEE Trans. Ind. Electron., vol. 59, no. 2,February 2012.

[12] D. B. Minh, V. D. Quoc, and P. N. Huy, "Efficiency Improvement of Permanent Magnet BLDC Motors for Electric Vehicles", Eng. Technol. Appl. Sci. Res., vol. 11, no. 5, pp. 7615–7618, Oct. 2021.

[13] Mahmouditabar;A. Vahedi;N. Takorabet,"Design and Analysis of Interior Permanent Magnet Motor for Electric Vehicle Application Considering Irreversible Demagnetization", 2020 International Conference on Electrical Machines (ICEM), Year: 2020 | Volume: 1 | Conference Paper | Publisher: IEEE.

[14] Guanghui Du;Wei Xu;Jianguo Zhu;Na Huang,"Power Loss and Thermal Analysis for High-Power High-Speed Permanent Magnet Machines",IEEE Transactions on Industrial Electronics, Year: 2020 | Volume: 67, Issue: 4 | Journal Article | Publisher: IEEE.

[15] Lezhi Ye;Mingguang Cao;Yupeng Liu;Desheng Li,"Multi-Field Coupling Analysis and Demagnetization Experiment of Permanent Magnet Retarder for Heavy Vehicles" IEEE Access Year: 2019 | Volume: 7 | Journal Article | Publisher: IEEE.